Available online at www.sciencedirect.com
SCIENCE DIRECT
Cement and Concrete Research 36 (2006) 371 – 383
Cement and Concrete Research

Deterioration of concrete in a hydroelectric concrete gravity dam and its characterisation

Ahmad Shayan [a,*], Jack Grimstad [b]

[a] ARRB Group Ltd, 500 Burwood Highway, Vermont South, Victoria, Australia
[b] Snowy Hydro, P.O. Box 332, Cooma, New South Wales, Australia

Received 21 January 2005; accepted 8 September 2005

Abstract

A hydroelectric concrete gravity dam in the Snowy Hydro network had shown signs of concrete distress in the form of cracking in some sections of the dam wall, and vertical movements in the wall, measured in routine surveys on the crest of the dam wall. Concrete elements of the associated power station had also shown some degree of distress in the form of cracking. Alkali-aggregate reaction (AAR) was considered among other mechanisms as a likely cause of cracking.

In order to investigate the main causes of cracking of the various elements of the power station and the dam wall, core samples ranging in length from 0.3 m to 10 m were extracted and investigated for the presence of AAR, its extent, likelihood of continuing reaction, residual expansion potential, and effect on the strength of concrete.

Results of the investigation showed that mild AAR was present in some sections of the wall of the power station but not in the floor, where drying shrinkage could have caused the cracking. Mild AAR was also present in sections of the dam wall with minor visible cracking, but it was stronger and more widespread in the badly cracked area. It was suggested that the walls of power station could be treated by appropriate surface coating to mitigate the progress of AAR, and the badly cracked portion of the dam wall be anchored to stabilise the vertical movement. Other portions of the dam wall did not appear to need treatment.

Keywords: Concrete dam; AAR; Residual alkali; Residual expansion; Strength

1. Introduction

The dam and power station investigated are a part of the Snowy Mountain Hydro-Electric System and are under the control of Snowy Hydro Ltd. Routine measurements of movements in the dam wall had revealed that some sections of the dam had shown as much as 13 mm movement over the 13 years of measurement between 1988 and 2001, i.e. 1 mm/year. Fig. 1A shows a general view of the dam wall observed from downstream, and graphical presentation of the movements measured on various locations on the crest. Regularly spaced surveillance points had been located on the crest and deformation markers (DM), suitable for the measurement of vertical movement, installed on the crest. Fig. 1B shows the total vertical movement at each DM location on the crest, over the measurement period, and Fig. 1C illustrates the change in the vertical movement over the same period for each measurement site. Note that the DM positions in Fig. 1B correspond to the same locations on the crest shown in Fig. 1A, i.e. locations of DM5–DM8 correspond to the spillway location. In order to maintain a high level of operational efficiency, in February 2002 Snowy Hydro Ltd. commissioned a review of this facility including the power generation components and the concrete structures. A preliminary inspection was first carried out on the power station and dam wall by the authors to ascertain their long-term durability. As a result, alkali-aggregate reaction (AAR) was suspected as the cause of deterioration of the concrete in the power station. Stronger evidence of AAR was observed on the dam wall, which were similar to previously reported cases of AAR in Australian dams [1–4].

AAR expansion and cracking can adversely affect the properties and performance of concrete structures, the extent of which would depend on the reactivity of aggregate, extent of

* Corresponding author.
E-mail address: ahmad.shayan@arrb.com.au (A. Shayan).

0008-8846/$ - see front matter © 2005 Elsevier Ltd. All rights reserved.
doi:10.1016/j.cemconres.2005.09.001

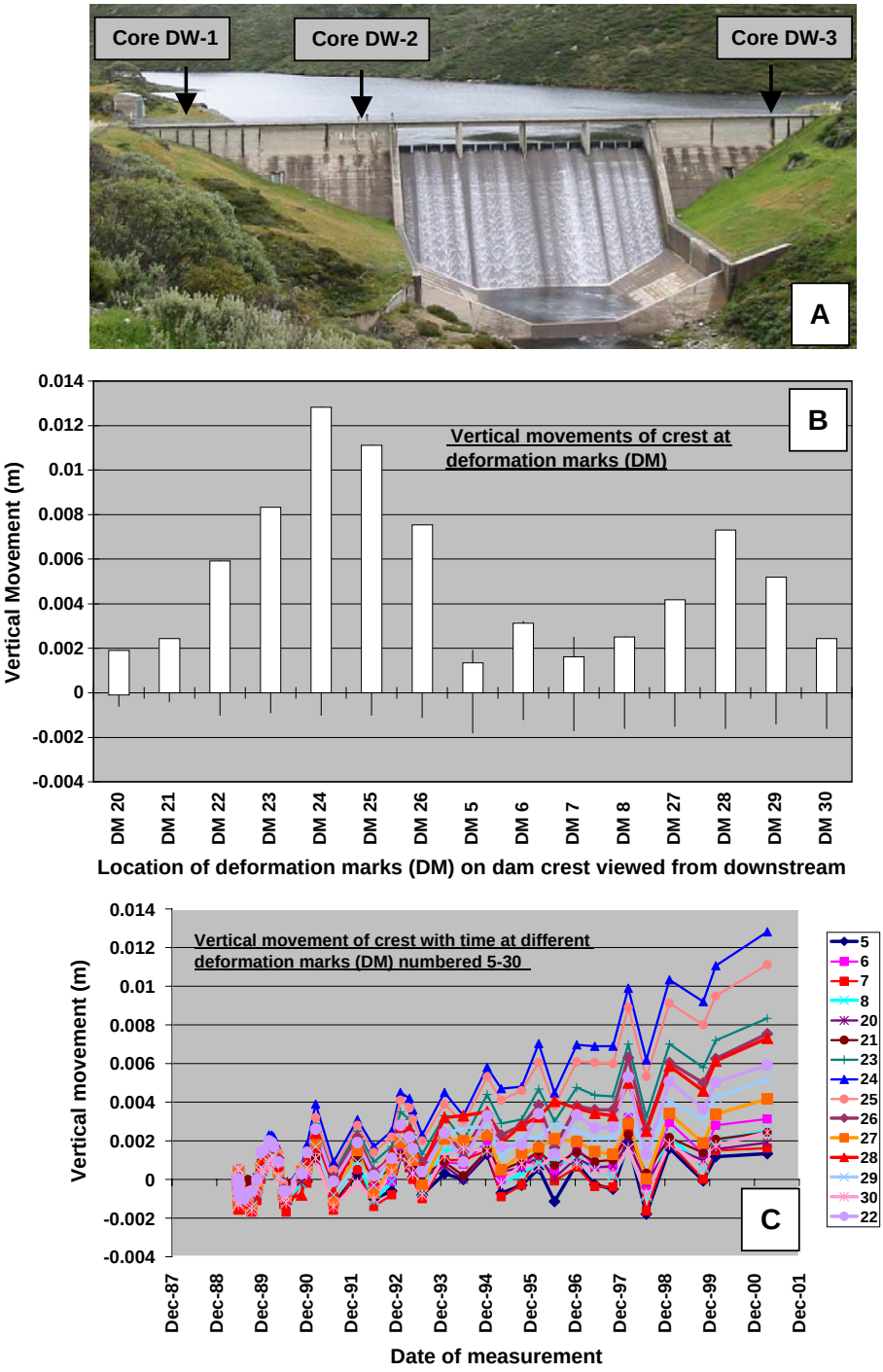

Fig. 1. General view of the dam from downstream (A), vertical movement of crest at different positions on the crest (B), and trend of expansion at each location with time (C).

reaction, type of element affected (mass concrete, reinforced, prestressed, etc.) and exposure conditions. The pattern of AAR cracking also depends on the type of element, being random (map-cracking) in plain and lightly reinforced concrete and directional in prestressed concrete. It is well known that steel reinforcement and applied stress have restraining effects on AAR expansion; the effects increasing with increased levels of reinforcement and applied stress [5]. At low levels of steel reinforcement, the AAR expansion could result in yielding failure of mild steel [6]. The compressive and tensile strength and elastic modulus of AAR-affected concrete were found to have been reduced by 60%, 50% and 30%, respectively, as a result of AAR, although the load bearing behaviour of the elements was not affected [6]. Other investigations have also provided evidence that most strength properties of AAR-affected concrete deteriorate compared to those of un-affected concrete [7–10].

Deterioration in the mechanical properties of concrete had caused serious problems in the Australian dams [1–4] which have all needed multi-million dollar rehabilitation. All these

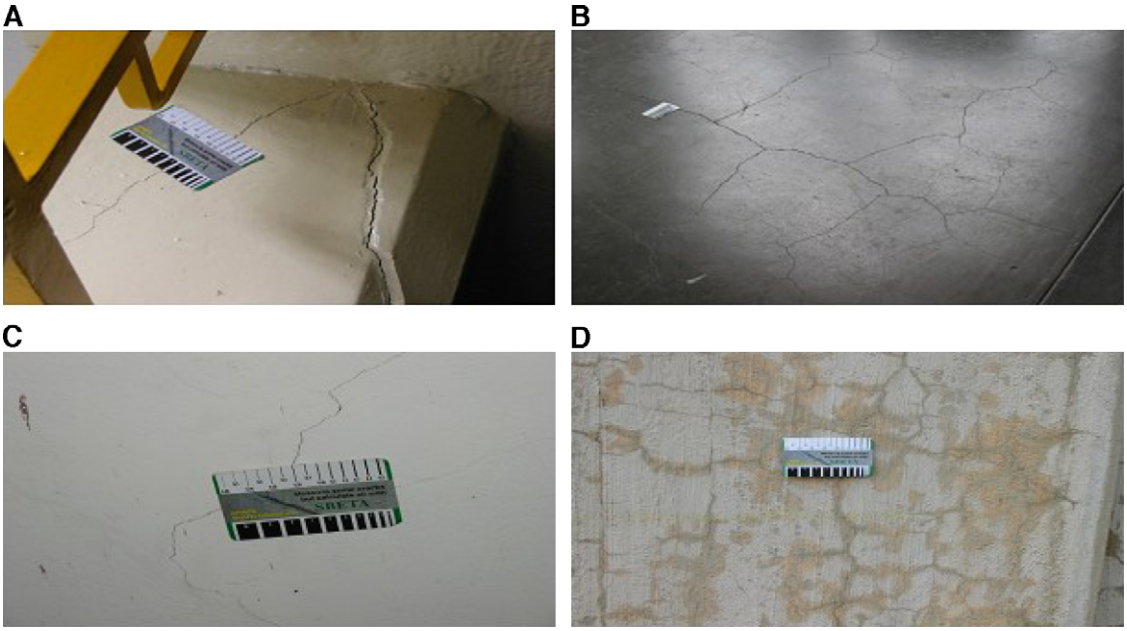

Fig. 2. (A) Cracking at the RHS of the beam of the assembly bay. (B) Crack pattern in the second slab in front of the Roll-a-door of the assembly bay. (C) Cracking observed on the staircase wall on the floor below the assembly bay floor. (D) Map-cracking pattern of an exterior column of the power station. Similar cracking is also present on the exterior walls.

Fig. 3. (A) Upstream view of the dam showing cracking of the block RHS of the spillway section. (B) Close up view of cracking of block D, RHS of spillway. (C) Cracking at the upper surface of block D.

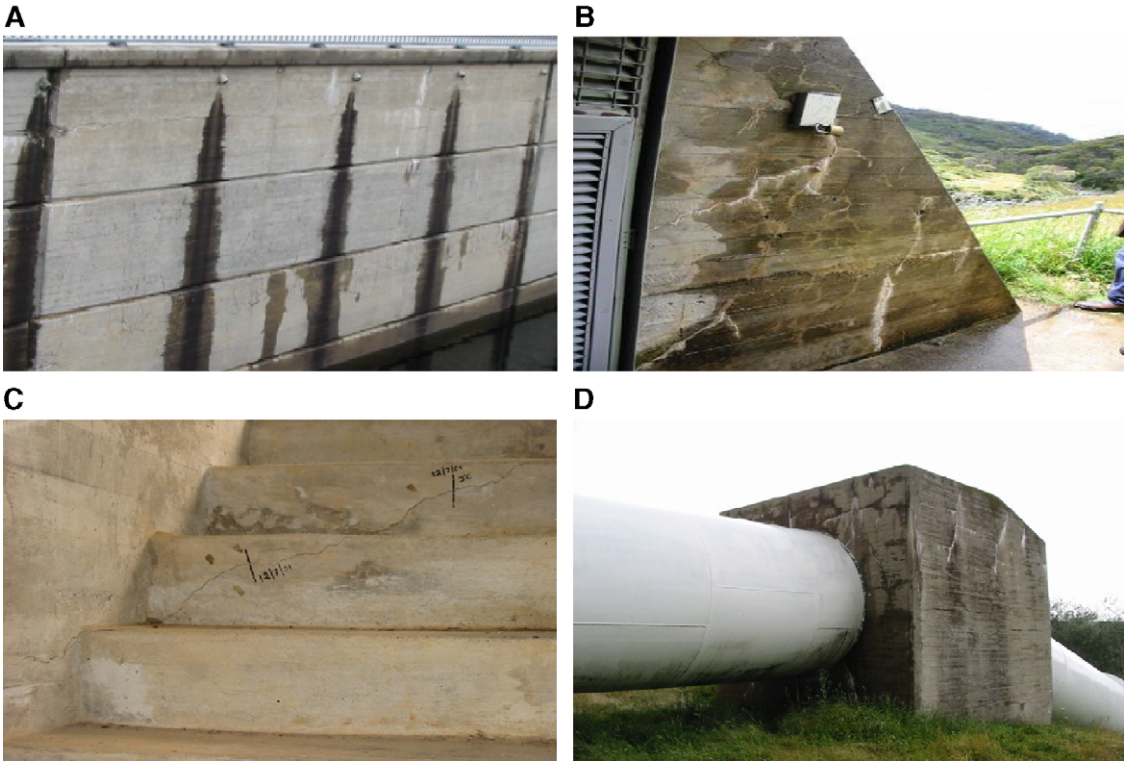

Fig. 4. (A) Milder cracking in the upstream face of the middle block to the left of the spillway. (B) Cracking of the buttress at the gallery entrance, due to AAR. (C) Cracking in the wall and staircase of the gallery—left entrance from downstream. (D) View of the pipeline anchor block exhibiting cracking.

dams contained slowly reactive aggregates. The investigation of the dam facilities under study in the current work is expected to generate information on the extent of work needed for their rehabilitation.

A number of tests were suggested for the investigation and characterisation of the damaged concrete. Photographs of concrete cracking in various parts of the structures are presented in Figs. 2–4. After the scope of the investigation was agreed on, cores were drilled from various parts of the power station and the dam wall. The scope of the work included characterisation of the present condition of the concrete, determination of the future expansion potential and recommendations for the repair of damage to the structure.

2. Materials and procedures

Short core samples were drilled from the floor of the assembly bay and the exterior wall of the power station. These cores were taken for diagnostic purposes to determine whether AAR is present in the concrete. Table 1 provides a description of these cores and their locations.

Long cores were taken from the crest of the dam wall to a depth of 10 m to determine the properties of concrete and its potential expansion in the future. The cores were all about 100 mm in diameter, and had a granitic gneissic aggregate as the coarse aggregate, varying in size from 5 mm to more than 75 mm in some cores.

Table 2 lists details of the cores drilled from the dam wall and their locations. The 10 m cores had broken into many pieces during the course of core drilling. The aggregate in the dam wall appeared to be very similar to that in the power station concrete. Each long core had a volume of about 80 l, and each drill hole was filled with a concrete mixture containing 25% by mass of cement of a proven fly ash to prevent AAR from occurring in the filling material.

In addition to the cores a batch of 120 kg of aggregate was collected from the site, which had remained on site since construction time. The aggregate was intended for testing in the

Table 1
List of cores taken from the power station (PS)

Core designation	Location	Core description
PS-1	Floor—Assembly Hall	Core length=275 mm. No sign of deterioration is evident.
PS-2	Floor—Assembly Hall	Length=320 mm. No sign of deterioration is evident.
PS-3	External column exhibiting micro-cracking	120 mm long with 3 pieces of steel bars. Most of the aggregate is <5 mm size.
PS-6	Floor 2—Workshop	225 mm long. No significant feature noted.
PS-7	Wall—Workshop	265 mm long. No visible sign of deterioration.
PS-8	Wall—Workshop	240 mm long. No unusual feature.
PS-9	Wall—Workshop	285 mm long. No unusual feature.

Table 2
List of cores taken from the dam wall (DW)

Core designation	Location and description
DW-1	First block on the far LHS of downstream face, looking from downstream. This block does not show cracking. There were 42 segments in the 10 m core length. No visual sign of deterioration was noted, except for a weak sign at depth of 7–10 m.
DW-2	Block immediately LHS of spillway, looking from downstream. This block shows significant cracking. There were 47 segments in the 10 m core length. Some segments showed visual signs of weak AAR rims.
DW-3	Block on the RHS of spillway, looking from downstream. This block shows mild microcracking. There were 36 segments in the core length. Weak visual signs of AAR noted in a few segments at 9–10 m depth.

laboratory to determine its reactivity and expansion potential, and to enable estimation of the maximum expansion that the aggregate could cause.

2.1. Test procedures

The cores were inspected and segments allocated to different examinations and tests. These included visual and petrographic examination; scanning electron microscopy (SEM) and energy dispersive X-ray (EDX) analysis; residual alkali content; residual expansion; and mechanical properties of concrete.

The aggregate was used for the following tests:

1. Accelerated mortar bar test (AMBT) according to the RTA Test Method T363, which is based on a paper by Shayan et al. [11], at four NaOH concentrations (0.7 M–1.0 M).
2. Concrete prism test (CPT) according to the ASTM C-1293 test method, at alkali contents of 1.0%, 1.25%, 1.5% and 1.8% by mass of cement.

The results of these tests allow judgement of the degree of reactivity of the aggregate for comparison with field observations of the concrete, and could be used to determine what level of future expansion could be expected.

3. Results

3.1. Visual examination of cores

Visual examination was conducted on all the cores from the power station and dam wall.

Observations made of the cores taken from the power station did not show strong signs of deterioration in the concrete (Table 1). Most AAR-affected structures exhibit considerable signs of reaction, and AAR products are often visible on fracture surfaces of the cores as rims on the aggregate or AAR gel covering the aggregate boundary and the adjacent mortar surface. AAR gel also occurs in some air voids near reacted aggregate pieces [1–4]. Observation of cores from the dam wall revealed only a few locations in cores DW-2 and DW-3 where such features could be seen in a mild form (Table 2). In a few locations some large voids next to the aggregate particles were only partially filled with AAR products. Details of these are given later in this paper.

It should be noted that in some medium- to coarse-grained rocks, such as the deformed granitic rock in the concrete of the dam wall, the AAR products can form within the intra-crystalline spaces in the aggregate, without being evident on the fracture surface. This type of formation would still exert expansive forces resulting in concrete cracking. More details about the microstructural features of the concrete and AAR are given in the following sections.

3.2. Petrographic examination of cores

Thin sections (75 × 50 mm) were prepared from the various cores taken from the power station and from every 2 m section of the long cores, for detailed petrographic examination. The results are given below in a condensed form, for both the power station cores and dam wall cores.

Except for minor variations, the coarse and fine aggregate components were very similar in all the cores. In some cases the aggregate pieces may exhibit more extensive alteration than in other cores, and some core segments may indicate a larger amount of crusher dust in the fine aggregate.

The coarse aggregate in the concrete was a deformed granitic rock, with distinct metamorphic features. It consisted

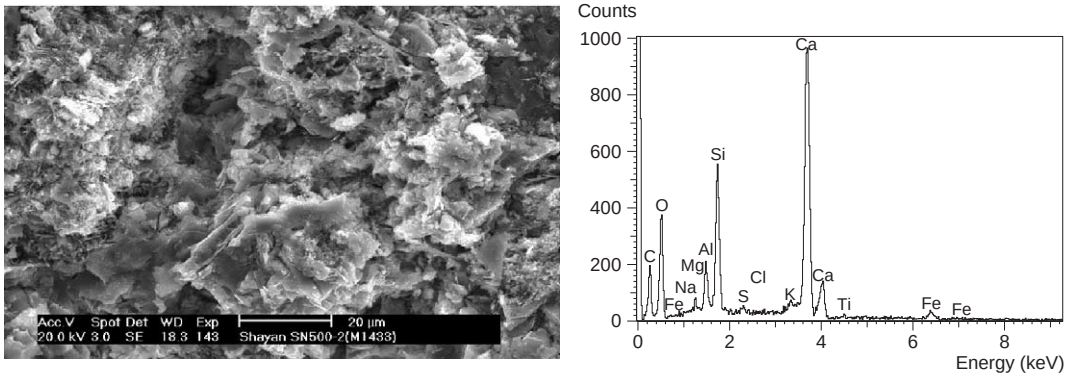

Fig. 5. SEM micrograph of cement paste and its EDX composition.

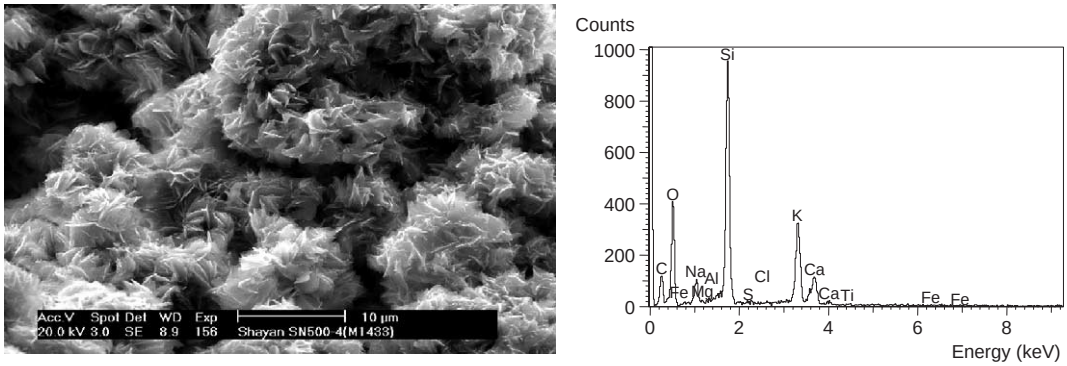

Fig. 6. Crystalline AAR product and its EDX composition.

of quartz, feldspar dominated by plagioclase, some microcline, biotite, altered micaceous materials, and in occasional sites quartz–feldspar intergrowth with a graphic texture.

The texture of the aggregate indicated that the rock has suffered a high degree of deformation. The quartz crystals showed varying degrees of strain with strong undulose extinction and sutured grain boundaries. In some places they showed signs of elongation and re-crystallisation into micro-crystalline quartz, which has formed at the borders of strained quartz grains, or completely occupied an adjacent area. Also, quartzitic features were seen in some zones. These features are probably randomly distributed in the structure, and showed variation from core to core. The strong pleochroic biotite showed characteristic cleavage, and was strongly fragmented and broken up, and intermingled with other crystals. The biotite appeared to have been altered to actinolite/tremolite in some locations, exhibiting a fibrous texture and high birefringence. In some other locations it was altered to fine fibrous crystals which were not pleochroic, but had high birefringence and were mixed with fine quartz crystals. The features of the quartz crystals strongly indicate this aggregate to be susceptible to AAR.

The sand fraction in the concrete consisted of a mixture of monocrystalline and polycrystalline quartz grains together with some feldspar and biotite fragments. The quartz, particularly in the polycrystalline grains showed varying degrees of undulose extinction. Some of the sand particles originate from the same rock as the coarse aggregate, indicating that crusher dust was mixed in the concrete. The fine aggregate may also be considered to be susceptible to AAR.

The cement matrix in the concrete appeared well hydrated. The extent of microcracking varied from core to core, reflecting the extent of external visual cracking. For instance, a core from the interior wall of the power station (core PS-7) did not show microcracking in the thin section, whereas in another core from the external column (core PS-3) microcracks originated from the fine or coarse aggregate boundaries and connected a number of air voids. Some aggregate pieces in the latter core showed microcracks partially around their boundary, from which multiple microcracks branched out into the cement matrix. Such microcracks were seen to extend to fine particle boundaries and traverse a part of their circumference. Some degree of AAR may have occurred in this concrete, and some of the microcracks appeared to contain AAR gel.

Microcracking in the deeper sections from core DW-1 (uncracked) was similar to that described above. In some parts AAR gel appeared to be present in microcracks within the aggregate and in its extension around the aggregate and into the cement matrix. This is the area that corresponds with the location of cracking in the gallery staircase (Fig. 3C).

However, in core DW-2 microcracking was more evident in the thin sections, but it varied along the core length. Some aggregate pieces showed considerable microcracking which branched into the cement matrix travelling to other aggregate boundaries or air voids. A large number of round air voids were present in the matrix, and some microcracks led to them. Some parts of microcracks adjacent to the aggregate pieces probably contained AAR gel. The cement paste at the boundary of some aggregate pieces appeared darker than the matrix, which may be due to the impregnation of the paste by AAR gel.

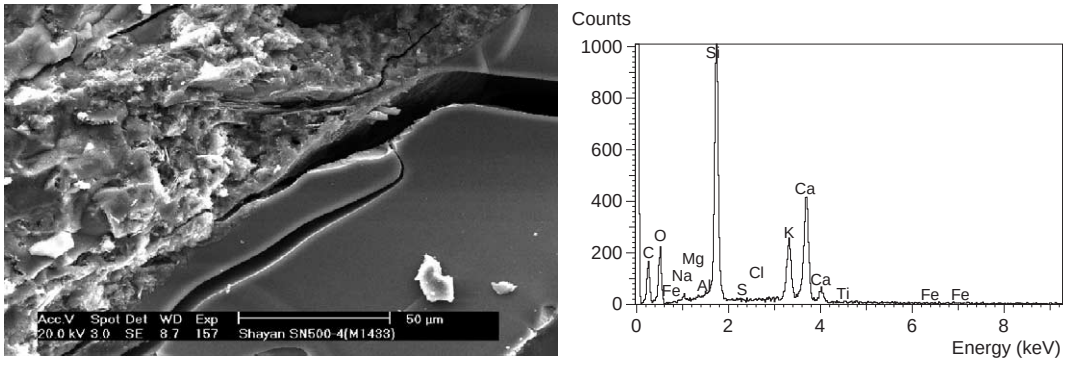

Fig. 7. Smooth AAR gel at aggregate boundary, and its EDX composition.

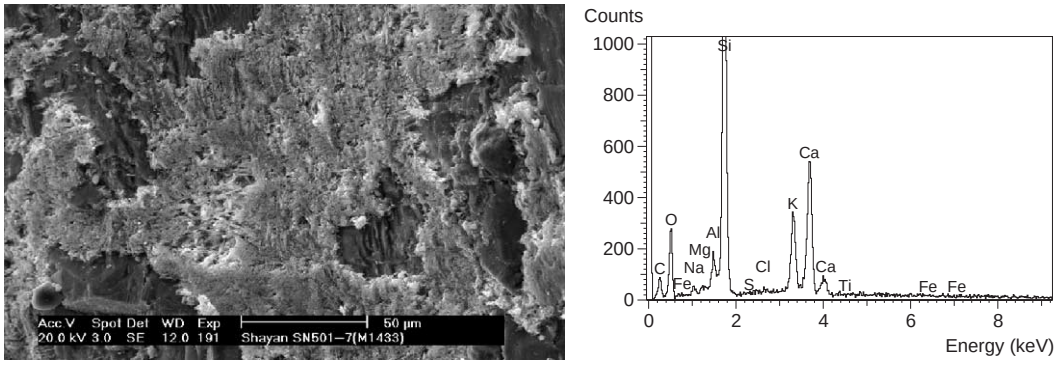

Fig. 8. AAR layer at crystal grain boundaries inside aggregate.

Petrographic features of core DW-3, taken from the mildly cracked block RHS of spillway were intermediate between those of core DW-1 and core DW-2. In two thin sections, a large aggregate piece (~30% of total area of section) appeared to be of the basic igneous group and not of the deformed granitic rock. Microcracking was generally mild in the sections observed for this core.

3.3. SEM/EDX examination

3.3.1. Cores from the power station

Cores PS-2 and PS-6 from the floors of the Assembly hall and Workshop, and cores PS-7 and PS-3, from the Workshop wall and Outside column, respectively, were examined by SEM and EDX analyses. A summary of the observations made on the cores is presented below.

Fig. 5 shows the microstructure of the hydrated cement phase in core PS-2 (floor of the Assembly Hall), and its composition, which is very low in alkali content (K and Na). Note that the cement hydrate is rich in Ca, and has a much lower Si content, as in the unhydrated cement. Detailed examination of the specimen did not reveal evidence of AAR in this core. The mortar matrix appeared porous in this specimen, and may indicate a high water/cement ratio in the original concrete, which would make it prone to excessive shrinkage. The cracking seen in the floor of the Assembly Hall may be due to excessive drying shrinkage.

Core PS-6 from the Workshop floor exhibited similar features. However, strong evidence of AAR was found in core PS-7, taken from the Workshop wall. Fig. 6 shows crystalline AAR products formed on an aggregate surface, and the composition indicated by the EDX spectrum is rich in Si, K and Na, unlike the hydrated cement phase. Fig. 7 shows a location where smooth AAR gel has formed at an aggregate boundary, and the composition is relatively richer in Ca due to contact with the hydrated cement (RHS). Similar K-rich AAR gel was found around some quartz grains, i.e. in the intra-crystal spaces between them. These features are very similar to those reported for AAR-affected structures elsewhere [12] and in Australia [1–4].

This type of AAR products were distinctly present in the core taken from the outside column of the power station, i.e. core PS-3, which shows map-cracking (Fig. 2D). Extensive reaction sites were noted in this core, and there is no doubt that the map-cracking in this column and adjacent walls, is due to AAR.

3.3.2. Cores from the dam wall

Five samples were examined from the 10 m long core, one specimen from each 2 m length. The composition of the hydrated cement paste in core DW-1 from the uncracked block, indicated higher contents of Si and Al in this cement compared to more modern cements, which could be attributed either to the composition of the older type cement or the fact that the granitic crusher fines had been used in the concrete.

AAR products were not detected in the specimens from the 0–4 m depth, but in several locations the concrete exhibited evidence of extensive carbonation, which could have masked AAR products, even if present. However, a number of

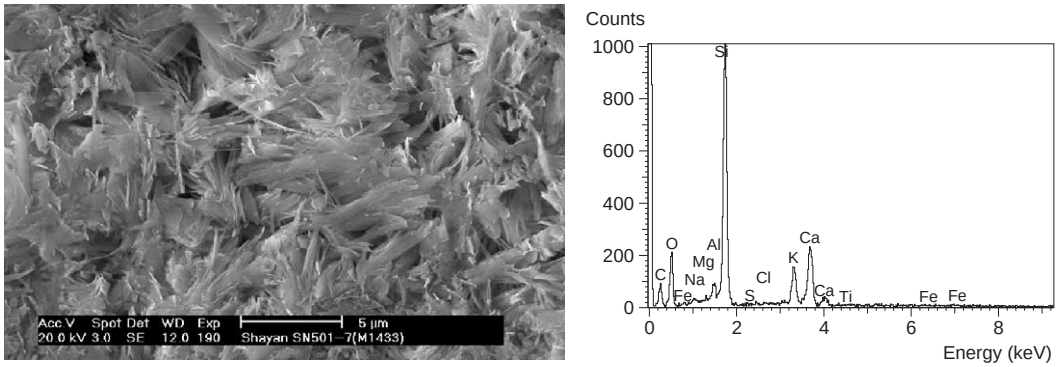

Fig. 9. Detail of AAR product shown in Fig. 7, showing compact crystals.

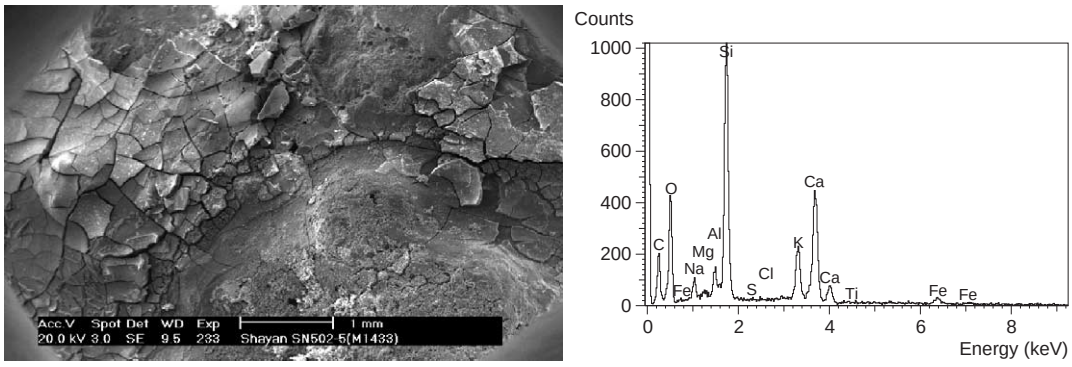

Fig. 10. AAR gel product covering large areas around aggregate and its EDX composition.

aggregate pieces in the core segment examined from 7 m depth contained AAR products. Fig. 8 shows a crusty layer of AAR products covering a large area of the aggregate fracture surface. At higher magnification this material appeared to be a compact crystalline AAR product as shown in Fig. 9. This AAR product seems to have formed the compact layer in the intra-crystalline spaces in the aggregate.

The identification of definite signs of mild AAR in the lower portions of core DW-1 agrees with the petrographic results, and corresponds to the cracked area of the gallery staircase.

Evidence of AAR was found throughout the whole 10 m length of core DW-2 which represents the visually damaged section of the dam wall. The AAR products had features similar to those already shown, but were more extensive. Some of the reaction sites covered the whole aggregate surface, as shown in Fig. 10 and had an alkali-rich composition. A large elongated space next to an aggregate particle was completely filled with alkali-rich AAR product, which is indicative of strong reaction. Other large areas of AAR gel were noted which appeared to have been leached, as indicated by the reduced alkali and increased Ca contents.

The concrete in some locations showed the presence of many round air bubbles, a few of which contained some loose clusters of ettringite (a calcium sulfoaluminate hydrate), but the latter occurrence is harmless.

Alkali-rich AAR products were also noted within some aggregate particles (Fig. 11). Such products generate expansive stresses within the aggregate particles which are then transferred to the surrounding cement paste and can cause cracking.

Data obtained for core DW-2 clearly shows the extensive nature of AAR in the cracked block to the left of spillway and is considered to be the cause of damage to the concrete in this area. The fact that these features were not evident in the petrographic thin sections arise because such evidence is easily removed during the cutting and polishing processes involved in the preparation of the sections.

Evidence of AAR was generally weak in core DW-3 from the mildly cracked block to the right of spillway, but strong evidence was noted in the 9–10 m depth. This may have arisen because of the strong carbonation noted in the higher parts of the concrete, which would have masked the AAR products.

The cement paste in core DW-3 was similar to that in the other cores from the dam wall. In this case AAR products were also noted at aggregate boundaries as well as within the aggregate at grain boundaries (Fig. 12). AAR gel was also noted lining some pores (Fig. 13). In very rare cases ettringite crystals were noted, sparsely growing into void spaces. The latter feature has no significance in this concrete. The large void, measuring 5–6 mm across, which was observed to have been lined by multiple layers of AAR gel (Fig. 13), illustrates one way in which AAR expansive forces are relieved, without causing damage. Overall, the observations made by SEM indicate a mild case of AAR in the block represented by core DW-3, which agrees with visual observations.

Despite the lack of strong visual signs of AAR, the products of the reaction formed in the dam wall were similar to those

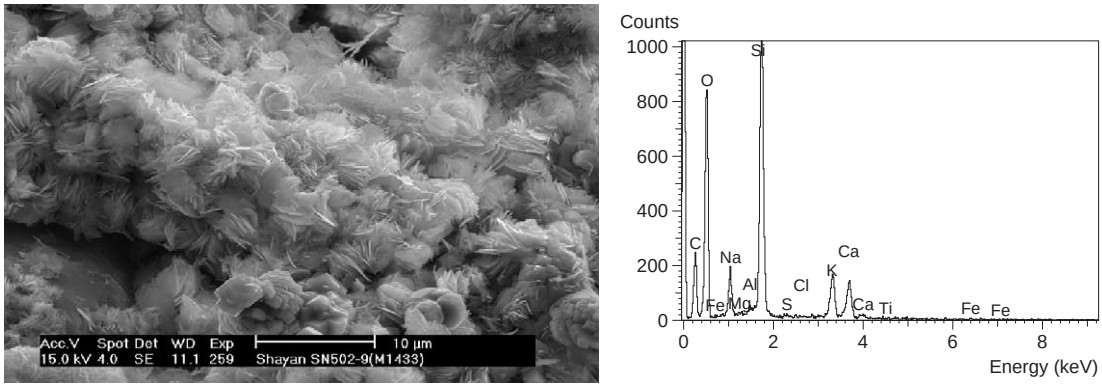

Fig. 11. Crystalline AAR product within aggregate and its EDX composition.

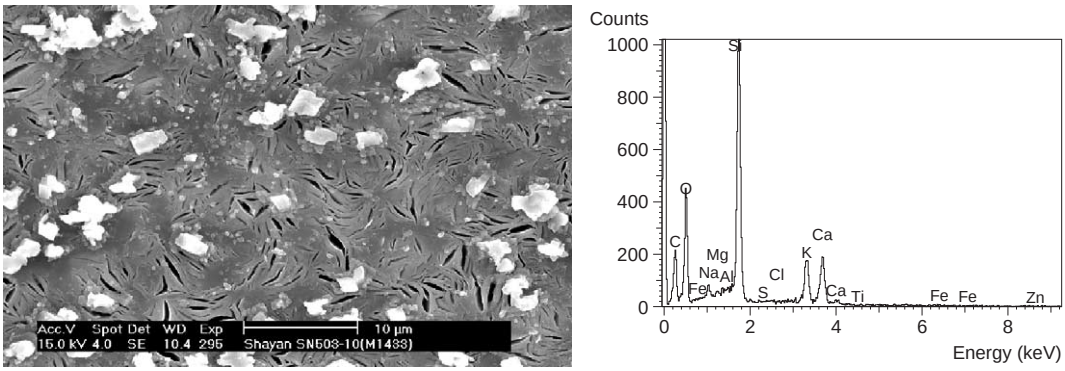

Fig. 12. Compact AAR layer within aggregate at crystal boundaries.

reported for another Australian dam that incorporated another slowly reactive deformed granitic rock [3].

3.4. Residual alkali content of concrete

To assess the tendency of concrete for further reaction, the residual soluble alkali content of the concrete was determined and the results are presented in Table 3. The method of alkali extraction was similar to those used elsewhere [3,4]. As the concrete is pulverised for this purpose, and includes a proportion of the aggregate phase, the alkali contribution from the aggregate phase was also determined for correcting the alkali content of the concrete.

For AAR to occur in this concrete, the total available alkali content needs to be at least 3.0 kg/m^3 for the deformed granitic rock. Table 4 shows that the residual amount of alkali is well below this limit. However, considering that some reaction has already taken place, values of greater than 2.0 kg/m^3 could be considered to indicate potential for further reaction. It should be noted that core PS-2 from the floor of Assembly Hall, which did not exhibit AAR, had a low residual alkali content of 0.92 kg/m^3, whereas core PS-7 from the wall of the power station, which had developed AAR, contained almost twice this amount. It is seen that the alkali contents of cores DW-1 and DW-3, from the uncracked and mildly cracked blocks, respectively, fall below this value, whereas core DW-2 could conceivably undergo further reaction. The lack of significant cracking in the floor areas of the power station, and in the uncracked blocks of the dam wall (core DW-1) could be the result of insufficient alkali in the concrete.

3.5. Residual expansion of concrete

The future expansion potential of the concrete could be estimated [3,4,13] by measuring the expansion of concrete cores under accelerated laboratory conditions, consisting of storage of core specimens, fitted with length measurement studs, at a temperature of 40 °C, 100% RH, and periodic length measurement. One core from each of the floor and wall of the power station, and five core segments from each of the three long cores were subjected to the measurement of residual expansion. The results are presented in Fig. 14. The data relate to 1 year of storage period, and it should be noted that the length measurements represent the maximum residual expansion potential of the concrete element. The field expansion may be smaller than the values obtained under laboratory conditions.

3.5.1. Cores from the power station

The core from the wall has continued to show a higher overall expansion than the core from the floor (Fig. 14). This is largely due to a higher initial expansion which could be related to water absorption by concrete and by the dehydrated AAR products in the former core. This is consistent with the observation of AAR products in the core sample taken from the wall and its absence in the concrete from the floor of the power station. Therefore, under wet conditions the walls of the

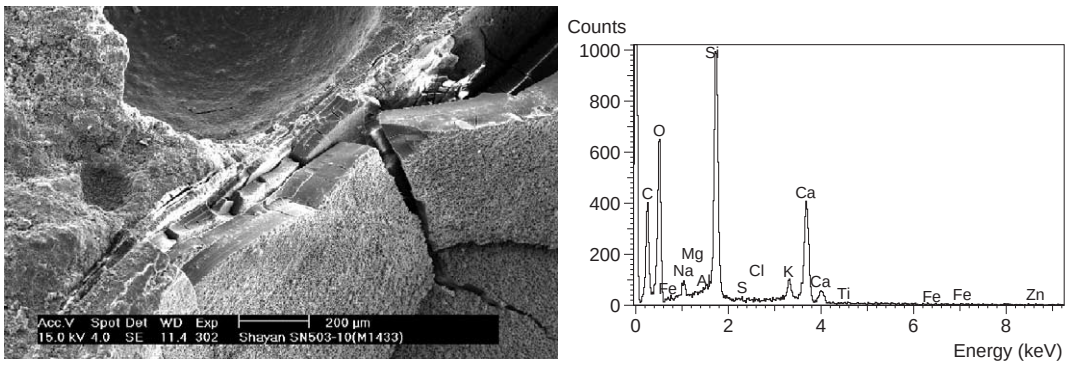

Fig. 13. AAR gel lining a large pore near reacted aggregate.

Table 3
Residual alkali content of concrete

Sample ID	Na_2O equiv[a] (%)	Dry density (kg/m^3)	Na_2O equiv (kg/m^3)	Corrected[b] Na_2O equiv (kg/m^3)
PS-2	0.058	2056	1.19	0.92
PS-7	0.106	1941	2.06	1.79
DW-1-1m	0.068	2351	1.61	1.34
DW-1-2m	0.088	2281	2.00	1.73
DW-1-3m	0.098	2322	2.27	2.00
DW-1-4m	0.104	2322	2.41	2.14
DW-1-5m	0.081	2334	1.88	1.61
DW-1-6m	0.074	2345	1.73	1.46
DW-1-7m	0.086	2267	1.95	1.68
DW-1-8m	0.069	2296	1.58	1.31
DW-1-9m	0.071	2286	1.63	1.36
DW-1-10m	0.071	2275	1.62	1.35
DW-2-1m	0.064	2247	1.43	1.16
DW-2-2m	0.077	2257	1.74	1.47
DW-2-3m	0.142	2285	3.24	2.97
DW-2-4m	0.109	2253	2.46	2.19
DW-2-5m	0.104	2221	2.31	2.04
DW-2-6m	0.104	2234	2.31	2.04
DW-2-7m	0.061	2324	1.42	1.15
DW-2-8m	0.071	2280	1.62	1.35
DW-2-9m	0.116	2328	2.70	2.43
DW-2-10m	0.066	2319	1.53	1.26
DW-3-2m-2	0.065	2258	1.46	1.19
DW-3-2m-3	0.066	2258	1.49	1.22
DW-3-3m	0.058	2258	1.31	1.04
DW-3-4m	0.076	2283	1.72	1.45
DW-3-5m	0.064	2307	1.47	1.20
DW-3-6m	0.060	2288	1.38	1.11
DW-3-7m	0.061	2294	1.39	1.12
DW-3-8m	0.062	2300	1.43	1.16
DW-3-9m	0.057	2338	1.32	1.05
DW-3-10m	0.091	2346	2.13	1.86
Aggregate	0.020	2715	0.54	

[a] % Na_2O equiv = %Na_2O + 0.658 (% K_2O).
[b] Correction for aggregate contribution is taken as 50% of the extracted alkali content of aggregate, based on the amount of rock in the concrete, i.e. 0.27 kg/m^3 Na_2O equiv.

power station would expand more than the floor. Ignoring the initial water absorption, the two expansion curves are almost parallel, indicating similar and small residual expansion values. Keeping the floor dry and applying a water proofing surface coating to the exterior of the wall would be able to prevent or reduce the expansion of these elements.

3.5.2. Cores from the dam wall

The expansion potential of the cores from the dam wall vary within each 10 m segment, as shown in the graphs presented in Fig. 14. The average expansion of the 10 m core segments at 1 year is calculated by taking the mean expansion for the five segments tested. The average water absorption for each segment is similarly calculated based on expansion at 30 days, and the difference is considered to be the residual AAR expansion potential of the core (Table 4).

The results are summarised as % expansion as well as expansion per meter and expansion per 20 m, assuming a height of 20 m for the dam wall. The results show that for the whole of the dam wall a maximum upward movement of 1.2–2.0 mm could be expected. However, two factors should be considered here. Firstly, that the stated expansion is related to the higher storage temperature in the laboratory at 100% relative humidity. It has been stated [14] that the field structure may only achieve around 50% of the residual expansion of cores measured in the laboratory, due to differences in the two environments and because of the confinement experienced by the structure compared to the freely expanding cores under laboratory conditions. Consideration of this issue would reduce the range of upward movement to 0.6–1.0 mm for the dam wall.

3.6. Mechanical properties of concrete

Core segments which were visually in a sound state were cut to 200 mm length (i.e. 100 × 200 mm cylinders) and capped at the two ends for compressive strength testing, after determination of their ultrasonic pulse velocity (UPV). Other similar core segments were cut for splitting tensile strength testing after the UPV measurements. Assuming a Poisson ratio of 0.2, the dynamic elastic modulus of the concrete was also calculated. The results are presented in Table 5.

The values of UPV and elastic modulus are acceptable and representative of sound concrete. It should be noted that the aggregate size and distribution varied considerably among core segments, and a strict strength comparison is not possible. Moreover, very large aggregate pieces in the specimens used for the splitting test resulted in unsatisfactory behaviour and instead of lengthwise splitting, the core was cracked in the transverse direction. This situation resulted in low strength values, which underestimate the actual strength of the concrete.

Generally, the strength of the concrete core segments is acceptable, and only in isolated cases such as in core DW-2 (1 m, 3 m, 5 m and 9 m) low values were noted, probably as a result of AAR damage. Particularly, the low elastic modulus of the core segment at 5 m was due to significant microcracking. As indicated in the Introduction section, these properties of concrete are sensitive to AAR effects. However, it should be noted that the core segments tested for strength were taken from the sound portions, whereas many fractures may have existed in the concrete, as revealed by the number of core segments in each drill core (although some of the pieces must have broken as a result of the drilling operation). The badly cracked concrete of block, represented by core DW-2, is an example, where the actual strength and integrity of the dam wall in that zone may have been

Table 4
Calculation of residual AAR expansion for the 3 cores from dam wall

Core designation	Average[a] expansion at 1 year (%)	Expansion due to water absorption 30 days (%)	Difference = residual AAR expansion		
			(%)	mm/m	mm/20 m
DW-1	0.021	0.013	0.008	0.08	1.6
DW-2	0.018	0.012	0.006	0.06	1.2
DW-3	0.018	0.008	0.010	0.10	2.0

[a] Average of 5 measurements made on core specimens from every 2 m core length.

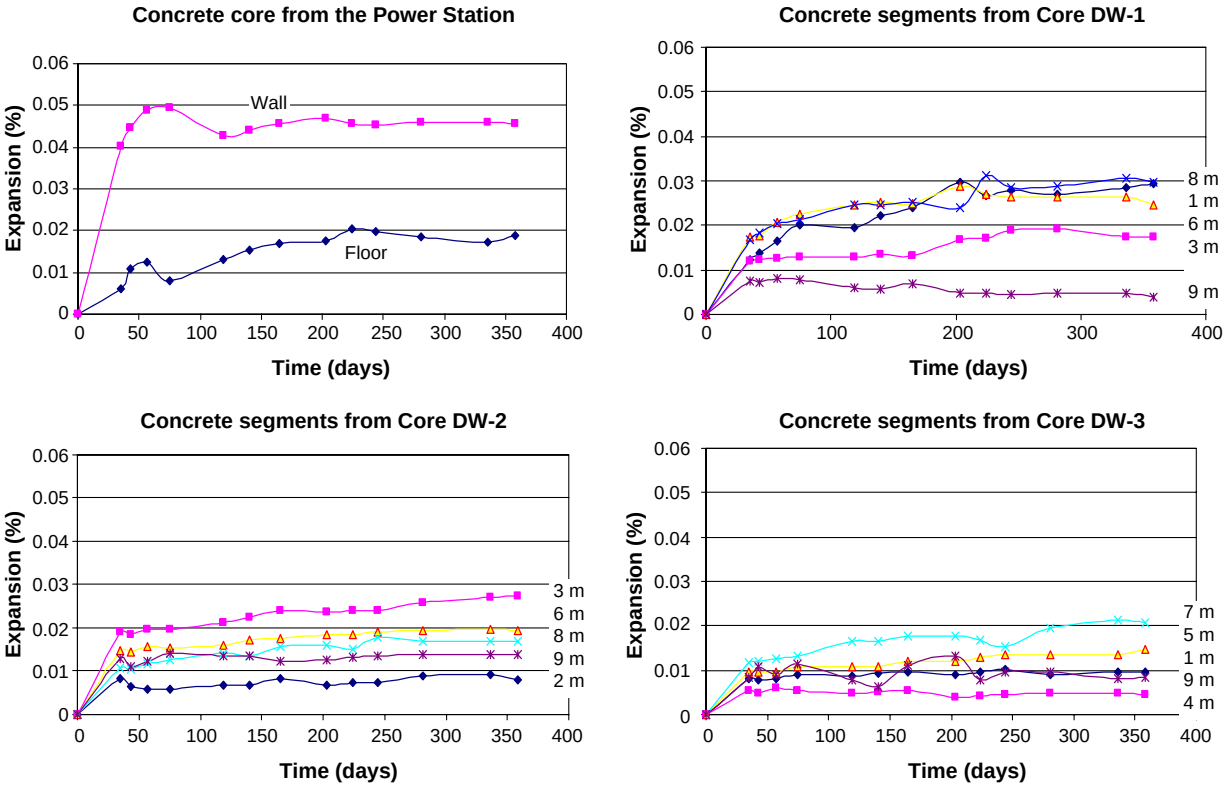

Fig. 14. Expansion of segments of concrete cores drilled from various parts of the structure, as indicated.

overestimated by the results of testing the sound portions of the core. The discontinuity of the concrete in cracked areas could be treated by anchorage of concrete in this limited area to restore its monolithic action. This anchorage could also be designed to confine the movement that is expected to arise from the residual expansion of the concrete. As stated in the Introduction, confinement by applying stress to concrete has a significant effect on suppressing AAR expansion.

3.7. Testing of aggregate

The bulk aggregate received from Snowy Hydro Ltd, in the form of 100 mm spalls, was crushed into 20 mm aggregate for concrete prism testing (CPT) according to the ASTM C-1293 test method for evaluation of its alkali-reactivity. A portion of this aggregate was further processed for testing by the accelerated mortar bar testing (AMBT), according to RTA T363 method.

Both tests were conducted at different alkali contents to assess the susceptibility of the aggregate to alkali, and its likely behaviour in the structures examined.

Fig. 15 shows the results of the AMBT method. In this test expansion values of greater than 0.10% at 10 days indicate reactive aggregate, and 0.10% or greater between 10 and 21 days, slowly reactive aggregate. Expansion values less than 0.10% at 21 days indicate non-reactive aggregate.

The results presented in Fig. 15 show that even at the lower alkali levels the aggregate behaves as a slowly reactive aggregate. This is in agreement with the results of the petrographic description which classed the aggregate as susceptible to alkali. The 0.70 M NaOH solution is equivalent to a total alkali content in the concrete of 5.2 kg Na_2O equiv. per cubic metre. The lowest limit of alkali for deleterious reaction of the aggregate is not known from these tests. However, the alkali content of the concrete is probably lower than this limit and further reaction does not appear likely in cores DW-1 and DW-3.

Fig. 16 shows the results of the CPT, for which the limit of deleterious expansion is 0.04% at 1 year. Based on the data for 1 year of measurement, deleterious expansion has occurred at cement alkali levels above 1.25% (5.25 kg alkali/m^3), leading to cracking of the specimens. The specimens containing 1.25% alkali may need longer than 1 year to develop deleterious expansion, as do some other similar slowly reactive aggregates [15]. These results indicate that portions of the dam that have not cracked must have used either a low alkali cement, or a low cement content in the concrete; the former being more likely as the strength which is related to the cement content was similar for the uncracked portions. The results also show that the aggregate has a high alkali tolerance, and uncracked portions of the dam are not likely to crack in the future due to AAR.

4. Conclusions

Laboratory testing of the aggregate used in the construction of the dam and power station has verified its slowly reactive nature.

Residual expansion measurements conducted on cores taken from various concrete elements have indicated that

Table 5
Strength properties of concrete cores

Core ID	Density, kg/m^3	UPV, m/s	$E_{dynamic}$ (ν=0.2), MPa	Compressive, MPa	Split tensile, MPa	Note on split test and $E_{dynamic}$
PS-2	2302				5.6	
PS-3	2346	4204	37,317	37.7		
PS-7	2320	4284	38,308		4.4	
PS-8	2356	4341	39,957	44.6		
DW-1-1m	2413	4180	37,941	38.1		
DW-1-2m	2329	4190	36,802		4.7	
DW-1-4m-a	2385	4682	47,054		5.3	
DW-1-4m-b	2385	4506	43,595	41.7		
DW-1-5m-a	2401	4509	43,922		5.0	
DW-1-5m-b	2439	4302	40,633	41.4		
DW-1-7m	2324	3994	33,370	32.0		
DW-1-8m	2333	3756	29,624		3.2	
DW-1-10m-a	2325	4565	43,602	29.7		
DW-1-10m-b	2325	4154	36,109		2.2	Transverse break along big aggregate
DW-2-1m-a	2323	4236	37,518	17.3	4.1	
DW-2-1m-b	2295	4346	39,013	31.1		
DW-2-3m-a	2341	3807	30,542	25.3		
DW-2-3m-b	2333				2.7	Split on one side only
DW-2-5m	2273	2967	18,006	25.7		Low elastic modulus due to significant microcracking
DW-2-6m	2279	4135	35,078		3.9	
DW-2-7m-a	2370	4589	44,919		3.5	
DW-2-7m-b	2370	3931	32,959	31.2		
DW-2-9m	2383	3853	31,843	25.4		
DW-2-10m	2361	4270	38,748		3.6	
DW-3-1m-a	2331	4410	40,796	38.4		
DW-3-1m-b	2305	4158	35,854		4.1	
DW-3-3m-a	2329	4266	38,144	27.6		
DW-3-3m-b	2310	3644	27,615		3.2	Transverse break along big aggregate
DW-3-5m	2356	4421	41,449		4.0	
DW-3-6m	2345			34.2		
DW-3-7m-a	2359	4402	41,128	24.7		
DW-3-7m-b	2339	4152	36,295		3.7	
DW-3-9m-a	2378	4525	43,811	20.9		
DW-3-9m-b	2369	4345	40,258		2.7	Transverse break along big aggregate

the concrete floor of the power station has very low residual expansion, and keeping it dry would prevent further expansion. The walls exhibited a larger potential for expansion under wet conditions, arising from the presence of partially dehydrated AAR products, but the application of a silane surface coating to the exterior of the walls would allow the concrete to dry further and suppress the expansion of these elements.

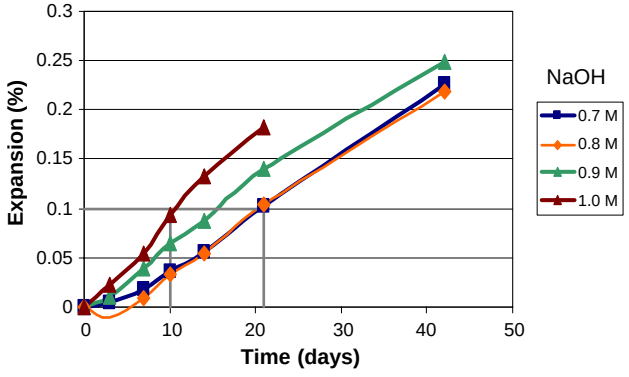

Fig. 15. AMBT results for the aggregate at the four NaOH concentrations indicated.

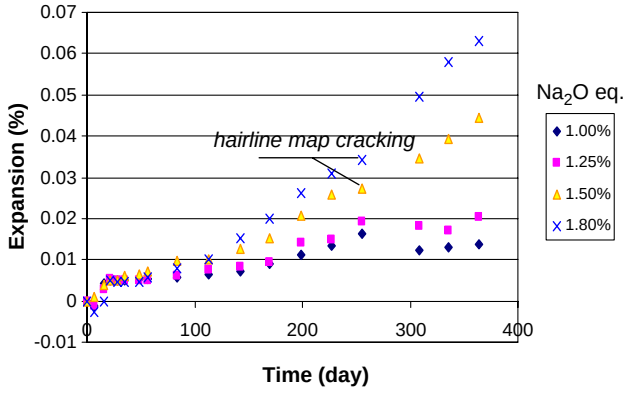

Fig. 16. CPT results for various concrete alkali contents.

The dam wall itself could be subjected to a total vertical expansion of 0.6–1.0 mm with a maximum of 1.2–2.0 mm. Appropriate method of managing this movement should be developed if this level of movement is of concern to the Snowy Hydro.

5. Suggested repair actions

It appears that the concrete floor in the power station is not exhibiting AAR, and may not need treatment. The exterior walls of the power station would need a breathable surface coating such as a water-repellent silane to prevent moisture ingress and allow the concrete to dry out. The interior walls may be treated with a surface coating appropriate for its current function.

The dam wall may need anchorage in the areas of badly cracked block. The uncracked and the mildly cracked blocks are not expected to need treatment. Details of anchorage could be arranged by companies specialising in the field, but it should consider the residual expansion potential of the concrete.

References

[1] A. Shayan, Int. J. Cem. Compos. Lightweight Concr. 10 (4) (1988) 259.
[2] A. Shayan, Cem. Concr. Res. 19 (1989) 434.
[3] A. Shayan, ANCOLD Bull. 112 (1999) 165.
[4] A. Shayan, R.E. Wark, A. Moulds, Proc. 11th Int. AAR Conf. June 2000, Quebec city, Canada, 2000, pp. 1383–1392.
[5] D.W. Hobbs, Alkali Silica Reaction in Concrete, Thomas Telford, London, 1988.
[6] M. Fujii, K. Kobayashi, T. Kojima, H. Maehara, in: P.E. Grattan Bellew (Ed.), Concrete Alkali Aggregate Reaction, Noyes Publications, New Jersey, USA, 1987, pp. 126–130.
[7] K. Ono, Proc. 8th Int. AAR Conf., Kyoto, Japan, 1989, pp. 647–658.
[8] W. Koyanagi, K. Rokugo, Y. Uchida, Proc. 9th Int. AAR Conf., London, UK, 1992, pp. 556–563.
[9] R.N. Swamy, Proc. CANMET, ACI Int. Workshop on AAR in Concrete, Dartmouth, Nova Scotia, 1995, pp. 293–310.
[10] K. Takemura, M. Ichitsubo, E. Tazawa, A. Yonekura, Proc. 10th Int. AAR Conf., Melbourne, Australia, 1996, pp. 410–417.
[11] A. Shayan, R.G. Diggins, I. Ivanusec, P.L. Westgate, Cem. Concr. Res. 18 (1988) 843.
[12] M. Regourd, H. Hornain and P. Poitevin, The alkali-aggregate reaction—concrete microstructural evolution, Proc. 5th Int. AAR Conf., Cape Town, South Africa, paper S252/352.
[13] M.A. Berube, A. Pedneault, J. Frenette, M. Rivest, Proc. CANMET/ACI Int. Workshop on AAR in Concrete, Dartmough, Novc Scotia, 1995, pp. 267–280.
[14] M. Tomita, T. Miyagawa, K. Nakano, Proc. 8th Int. AAR Conf., Kyoto, Japan, 1989, pp. 779–784.
[15] A. Shayan, Concrete in Australia, 2001, pp. 24–26 (June–August 2001 issue).